International Orthopaedics (SICOT) (2010) 34:1341–1349
DOI 10.1007/s00264-009-0946-3

ORIGINAL PAPER

Enhanced bone formation in large segmental radial defects by combining adipose-derived stem cells expressing bone morphogenetic protein 2 with nHA/RHLC/PLA scaffold

Wei Hao · Jinlei Dong · Ming Jiang · Junwei Wu · Fuzhai Cui · Dongsheng Zhou

Received: 1 November 2009 / Revised: 14 December 2009 / Accepted: 20 December 2009 / Published online: 7 February 2010

Abstract In this study, rabbit adipose-derived stem cells (rASCs) were isolated, cultured in vitro, and transfected with recombinant adenovirus vector containing human bone morphogenetic protein 2 (Ad-hBMP2). These cells were combined with a nano-hydroxyapatite/recombinant human-like collagen/poly(lactic acid) scaffold (nHA/RHLC/PLA) to fabricate a new biocomposite (hBMP2/rASCs-nHA/RHLC/PLA, group 1) and cultured in osteogenic medium. Non-transfected rASCs mixed with nHA/RHLC/PLA (rASCs-nHA/RHLC/PLA, group 2) and nHA/RHLC/PLA scaffold alone (group 3) served as controls. Scanning electron microscope (SEM) demonstrated integration of rASCs with the nHA/RHLC/PLA scaffold. Quantitative real-time RT-PCR analyses of collagen I, osteonectin, and osteopontin cDNA expression indicated that the osteogenic potency of rASCs was enhanced by transfection with Ad-hBMP2. After in vitro culture for seven days, three groups were implanted into 15-mm length critical-sized segmental radial defects in rabbits. After 12 weeks, radiographic and histological analyses were performed. In group 1, the medullary cavity was recanalised, bone was rebuilt and moulding was finished, the bone contour had begun to remodel and scaffold was degraded completely. In contrast, bone defects were not repaired in groups 2 or 3. Furthermore, the scaffold degradation rate in group 1 was significantly higher than in groups 2 or 3. In summary, after transduction with Ad-hBMP2, the osteogenesis of rASCs was enhanced; a new biocomposite created with these cells induced repair of a critical bone defect in vivo in a relatively short time.

Wei Hao, Jinlei Dong and Ming Jiang contributed equally to this article.

W. Hao · J. Dong · J. Wu · D. Zhou (✉)
Department of Orthopaedics & Traumatology,
Provincial Hospital affiliated to Shandong University,
324 Jingwuweiqi Road,
Ji'nan 250021 Shandong, People's Republic of China
e-mail: sdgkxh@163.com

W. Hao
Department of Spinal Cord Injury,
General Hospital of Ji'nan Military Area,
Ji'nan, People's Republic of China

M. Jiang
Department of Stomatology,
General Hospital of Ji'nan Military Area,
Ji'nan, People's Republic of China

F. Cui
Biomaterials Laboratory, Department of Materials Science and Engineering, Tsinghua University,
Beijing, People's Republic of China

Introduction

The concept of bone tissue engineering has been widely accepted and is relatively far advanced in clinical applications for repair of large bone defects resulting from trauma or tumour resection, especially when the limited extent of autogeneic bone harvest is considered. In bone tissue engineering, biocompatible, osteoconductive and osteoinductive properties of bioengineering reconstructions should be considered. Three aspects including seed cells, bone osteoinductive proteins, and three-dimensional (3D) scaffold are involved and should be integrated during the fabrication process.

Mesenchymal stem cells (MSCs) such as bone marrow MSCs (BMSCs) or adipose-derived MSCs have been proven to differentiate into osteogenic lineage and have been widely used in bone tissue engineering as seed cells

[1–3]. Compared with BMSCs, adipose-derived stem cells (ASCs) have the similar multilineage differentiation capacity, but are easier to obtain, carry relatively lower donor site morbidity, and are available in larger numbers [4]. All these characteristics have made ASCs a seed cell source of interest and these cells have been shown to possess good osteogenic potency at ectopic and orthotopic sites [2, 3, 5].

Before combination with porous scaffolds, extensive in vitro culture of MSCs is usually necessary to provide adequate cell numbers. Unfortunately, the osteogenic potential of MSCs is decreased with increased passages after prolonged in vitro culture, which may lead to attenuation of in vivo bone-forming capacity [6]. Genetic enhancement of MSCs to express osteoinductive cytokines such as bone morphogenetic protein 2 (BMP2) could potentially increase their osteogenic capacity and induce and recruit MSCs from surrounding tissues to participate in new bone formation [7, 8]. This may shorten the in vitro culture time, allowing for potential application in clinical cases with limited time available before operation.

Synthetic biomaterials that serve as scaffolds also play an important role in bone tissue engineering. These biomaterials provide three-dimensional space for cell ingrowth and extracellular matrix formation and structural support for the newly formed bony tissue. Hydroxyapatite (HA) has a composition and structure very similar to natural bone mineral. However, clinical applications of HA have been limited because of brittleness and difficulty of shaping [9] and the relatively slow degradation rate [10]. Compared with traditional micro-sized ceramic materials, nano-sized HA is of current interest because it possesses some special properties, including large specific surface area and excellent biodegradability, biological activity, protein adsorption, and osteoblast adhesion [11–13].

Based on the biomimic mechanism of the unique structure of HA/collagen in natural bone, we designed a novel scaffold that we call nano-hydroxyapatite/recombinant human-like collagen/poly(lactic acid) (nHA/RHLC/PLA). The scaffold was fabricated by assembling collagen molecules and nano-HA into mineralised fibrils, which were then incorporated with poly(lactic acid) (PLA) to enhance mechanical properties. Related experiments have already demonstrated good bioactivity, biocompatibility and biodegradation rate of this scaffold [14–17].

In this study, rabbit ASCs were genetically modified to express human BMP2 (hBMP2). The nHA/RHLC/PLA was used as a carrier for the transfected ASCs and their osteogenic differentiation was analysed. Finally, a rabbit model with a 15-mm length critical-sized segmental radial defect was used to demonstrate the enhanced bone defect repair by hBMP2 genetically-modified ASCs combined with nHA/RHLC/PLA.

Material and methods

Harvest of rabbit adipose-derived stem cells (rASCs)

Approval was obtained by the Institutional Animal Review Committee of the Provincial Hospital affiliated to Shandong University before animal studies were begun. The isolation of rASCs was performed as previously described [18], and cells were cultured in medium containing DMEM, 10% foetal bovine serum (FBS), 100 μ g/ml penicillin and 100 μ g/ml streptomycin. At confluence, cells were passaged with 0.25% trypsin/EDTA and replated at 1:3 dilution.

Construction of recombinant adenovirus vector containing human BMP2 (Ad-hBMP2)

The hBMP2 cDNA fragment from plasmid pIRES2-EGFP-BMP-2 (kindly provided by Dr. De-bo Zou, Qian Fo Shan Hospital, Shandong Province, China) was cloned into the pShuttle 2 vector of Adeno-X™ Expression System 1 (Clontech, Takara Bio Company). The hBMP2 expression cassette was subcloned into the Adeno-X Viral DNA. After transformation into *E. coli*, the purified recombinant adenovirus vector was linearised and transfected into HEK 293 cells. Replication-defective adenoviruses were produced and purified. Plaque assays were performed to determine the viral titer. Recombinant adenovirus containing enhanced green fluorescence protein (Ad-EGFP) was constructed using the same procedure.

hBMP2 gene transfection into rASCs and combination with nHA/RHLC/PLA scaffold

Briefly, rASCs of passage 3 were prepared and used as target cells for gene transfection. The transfection efficiency of the rASC cells was evaluated using Ad-EGFP. In a pilot study, Ad-EGFP at multiplicities of infection (MOI, pfu/cell) of 100, 200, 300, 400, and 500 was transfected into rASCs and cultured overnight. The transfection efficiency was determined based on the percentage of fluorescent cells. A MOI of 400 provided the highest transfection efficiency (Fig. 1) and flow cytometry studies demonstrated minimal apoptosis at this MOI (data not shown).

The rASCs at 90% confluence were transfected with Ad-hBMP2 at 400 MOI for two hours and then the media was changed. After 24 hours, cells were seeded into the scaffolds at 2×10^6 cells/ml and cultured for four hours at 37°C in 5% CO_2 to produce genetically-modified composites (hBMP2/rASCs-nHA/RHLC/PLA). The constructions were removed to new wells and covered with osteogenic medium containing DMEM, 10% FBS, 0.1 μ M dexamethasone (Sigma, St. Louis, MO, USA), 50 μ g/ml ascorbic

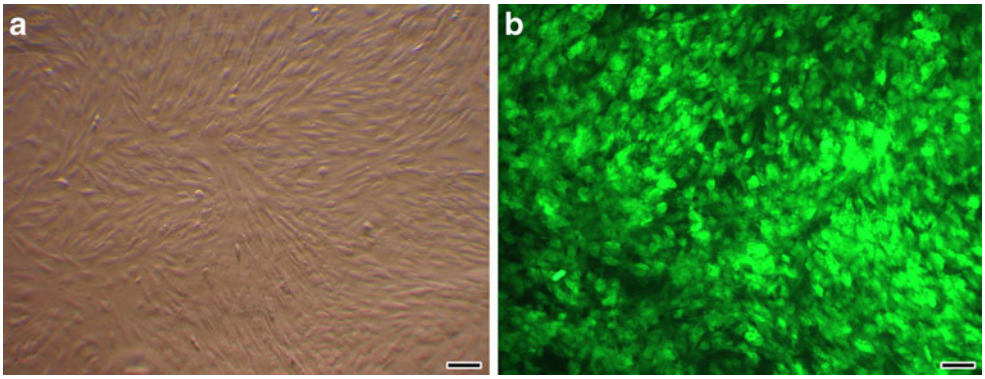

Fig. 1 Representative fluorescence of rabbit adipose-derived stem cells (rASCs) transfected with adenovirus containing enhanced green fluorescence protein (Ad-EGFP) at a multiplicity of infection (MOI) rate of 400. Scale bar 50 μm. **a** No obvious cell toxicity was observed. **b** >90% rASCs expressed EGFP

acid-2-phosphate (Sigma, St. Louis, MO, USA), 10 mM β-glycerophosphate (Sigma, St. Louis, MO, USA), 100 μ g/ml penicillin, and 100 μ g/ml streptomycin. The non-transfected rASCs mixed with scaffold (rASCs-nHA/RHLC/PLA) using the same process served as a control.

Quantitative real-time RT-PCR analysis

At one, four, and seven days post-transfection, three samples of each group were analysed to determine levels of expression of osteogenic-specific genes, including collagen I (Col I), osteonectin (ON), and osteopontin (OP). Total RNA was obtained by using Trizol reagent (Invitrogen Life Technologies, Carlsbad, CA, USA) and was reverse transcribed to cDNA. The real-time PCR assay volume of 25 μL contained 1 μL cDNA, 10 μM gene-specific primers, 2x SYBR Premix Ex Taq™ (TaKaRa Biotechnology Co., Ltd., Dalian, China), and 50x ROX Reference Dye was incubated in an ABI 7500 Real-Time Thermocycler (Applied Biosystems, Foster City, CA, USA). After an initial denaturation at 95°C for 15 min, 45 cycles of 94°C for 15 s, 58°C for 30 s, and 72°C for 45 s were applied. β-actin was used as an internal control to evaluate total RNA input. The levels of Col I, ON, and OP cDNA were calculated by using the comparative threshold-cycle (Ct) method [19]. The efficiency of each assay was calculated using the formula $E = 10-1/slope$. Primer sequences used in quantitative real-time PCR were β-actin sense, 5′-CCTTCCTGGGCATGGAGTCCTGG-3′; β-actin antisense, 5′-GGAGCAATGATCTTGATCTTC-3′; Col I sense, 5′-TTCTATTGGTCCCGTCGGT-3′; Col I antisense, 5′-GCTGAGTCTCAGGTCGCG-3′; OP sense, 5′-CACC ATGAGAATCGCCGT-3′; OP antisense, 5′-CGTGACTTT GGGTTTCTACGC-3′; ON sense, 5′-AGGAAGTAGT GGCCGAAAACC-3′; and ON antisense, 5′-TGTGGGA CAGGTACCCGTC-3′.

Observation of cell-scaffold composites

After seven days, the osteogenic medium was removed and the cell-scaffold composites were washed with PBS, fixed with 2.5% glutaraldehyde, dehydrated through a graded series of ethanol, and critical point dried. After being fixed onto scanning electron microscopy aluminum stubs, samples were sputter coated with gold and observed under a scanning electron microscope (SEM, Hitachi High-Technologies Corp., Tokyo, Japan). The scaffold alone was processed as a control.

In vivo implantation

After in vitro culture for seven days, the constructs were ready for in vivo implantation. Twenty Japanese white rabbits were used for the orthotopic defect repair study. Rabbits were anaesthetised. An approximately 2.5-cm incision was made over the radius and the tissues overlying the middle diaphyseal radius were dissected. A 15-mm segmental osteoperiosteal defect was created in the radius with a mini-oscillating saw bilaterally. After resection, the defect site was implanted with hBMP2/rASCs-nHA/RHLC/PLA (group 1, n=6), rASCs-nHA/RHLC/PLA (group 2, n=6), and nHA/RHLC/PLA (group 3, n=4), with untreated bone defect as an additional control (n=4). At six and 12 weeks postoperatively, three rabbits from groups 1 and 2 and two rabbits from group 3 and the untreated control group were harvested and the radii with ulnas were explanted and fixed with 10% formalin for further analyses.

Radiographic analyses

At six and 12 weeks postoperatively, the radii with ulnas were harvested and imaged. Each radiograph was examined by two independent observers and given a score based on a standardised scoring system (Table 1).

Histological analyses

After being fixed, decalcified, dehydrated, and embedded in paraffin wax, the tissues were cut into 7-μm sections and stained with haematoxylin and eosin (HE). For morphometric analysis, five sequential sections per implant were selected for evaluation under low magnification, allowing

Table 1 Radiographic scoring system

Classification		Score
Bone formation	None	0
	25% of defect	1
	50% of defect	2
	75% of defect	3
	Full	4
Persistence of the fracture line	Full fracture line	0
	Partial fracture line	2
	Absent fracture line	4
Bone remodelling	None	0
	Intramedullary canal	2
	Full cortex	4

coverage of the entire implant. Using a Leica-Qwin 3.2 Image Analysis System (Leitz DMRD, Leica Microsystems, Inc., Bannockburn, IL, USA), all slides were evaluated by two independent observers to identify the type of bone tissue or scaffolds. The extent of bone formation or residual scaffold was indicated by the percentage of the bone tissue area or scaffold area within the defect site and an average value was calculated for each implant. Data were then averaged across all implants within each group.

Statistical analyses

All quantitative data were expressed as mean and standard deviation. The relative expression level of target genes, percentage of bone formation, and percentage of residual scaffold were compared by ANOVA. Radiographic scoring data were processed as ordinal ranking and analysed with the Mann-Whitney U test. Level of statistical significance was defined as $p<0.05$.

Results

Osteogenic differentiation of rASCs combined with nHA/RHLC/PLA

The rASCs were efficiently transfected with adenovirus vectors, and rASCs that expressed hBMP2 were created. hBMP2/rASCs cells and untransfected cells were grown in the presence of nHA/RHLC/PLA. By using quantitative real-time RT-PCR, expression of Col I, ON, and OP was quantified and compared between cells transfected with hBMP2 and untransfected cells.

As shown in Fig. 2, osteogenic specific gene expression increased over a one-week period. From day four to day seven, the hBMP2/rASCs-nHA/RHLC/PLA cells demonstrated significantly higher gene expression than the rASCs-nHA/RHLC/PLA cells ($p<0.05$, $n=3$). This indicated that the hBMP2-modified rASCs were incorporated into the scaffold and exhibited enhanced differentiation towards osteogenic lineage. As shown in Fig. 3a, b, the scaffold has a highly interconnected porous structure with pore sizes

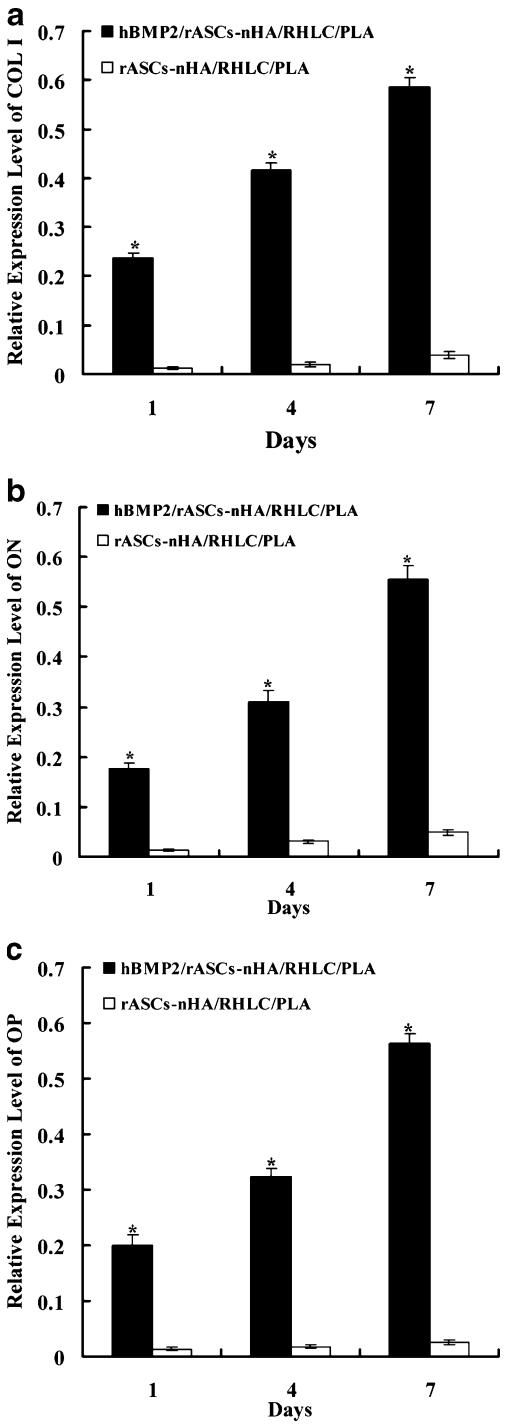

Fig. 2 Relative expression levels of COL I (**a**), ON (**b**) and OP (**c**). *$p < 0.05$ statistically significant compared with rASCs-nHA/RHLC/PLA (group 2)

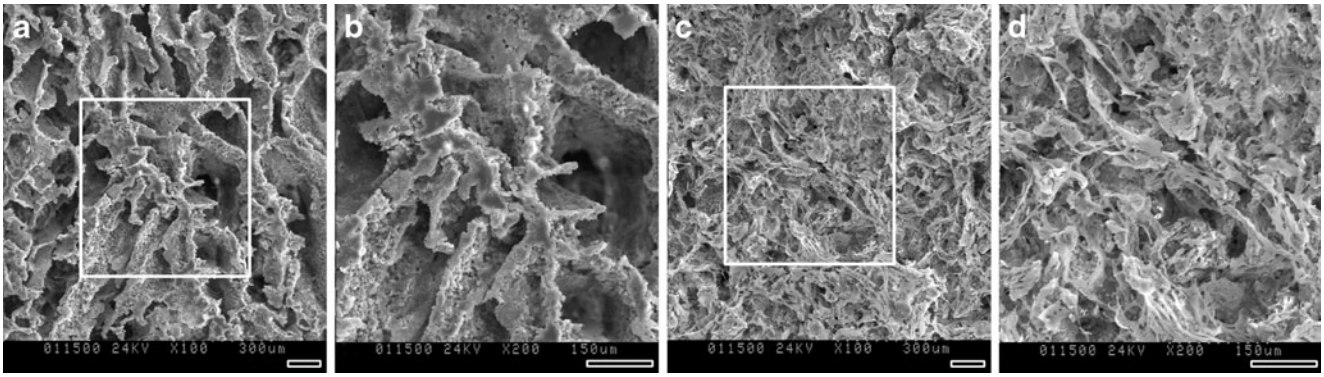

Fig. 3 SEM observations. Scale bar 100 μm. **a** nHA/RHLC/PLA porous scaffold. **b** Magnified view of the *white rectangle frame* from (**a**). **c** Co-culturing of rASCs combined with nHA/RHLC/PLA porous scaffold under osteogenic medium after seven days. **d** Magnified view of the *white rectangle frame* from (**a**)

that range from 10 μm to about 300 μm. After in vitro culture for seven days, the rASCs exhibited a fibroblast-like appearance similar to rASCs grown in a culture dish. The cells adhered evenly onto the surface of the scaffold and into the inner pores (Fig. 3c, d).

Radiographic analyses

Japanese white rabbits were used for the orthotopic defect repair study. The defect site was implanted with hBMP2/rASCs-nHA/RHLC/PLA in group 1 animals, rASCs-nHA/RHLC/PLA in group 2 animals, and scaffold alone in group 3 rabbits. Untreated bone defects served as an additional control. Six weeks after implantation, a radiopaque area of new bone formation was observed in the defect field in group 1, although some radiolucent area was still seen (Fig. 4a). At 12 weeks post-surgery, bone cortex was formed at the defect site and the medullary cavity was recanalised and completely reconnected with adjacent normal bone tissues in group 1. The bone rebuilding and molding was finished and the bone contour had begun to remodel (Fig. 4b). In contrast, no apparent evidence of osteogenesis was present in group 2 except for a cloudy shadow of scaffolds at six and 12 weeks postoperatively (Fig. 4c, d). Furthermore, hardened cutting ends appeared after 12 weeks at the defect site (Fig. 4d). Analyses of the

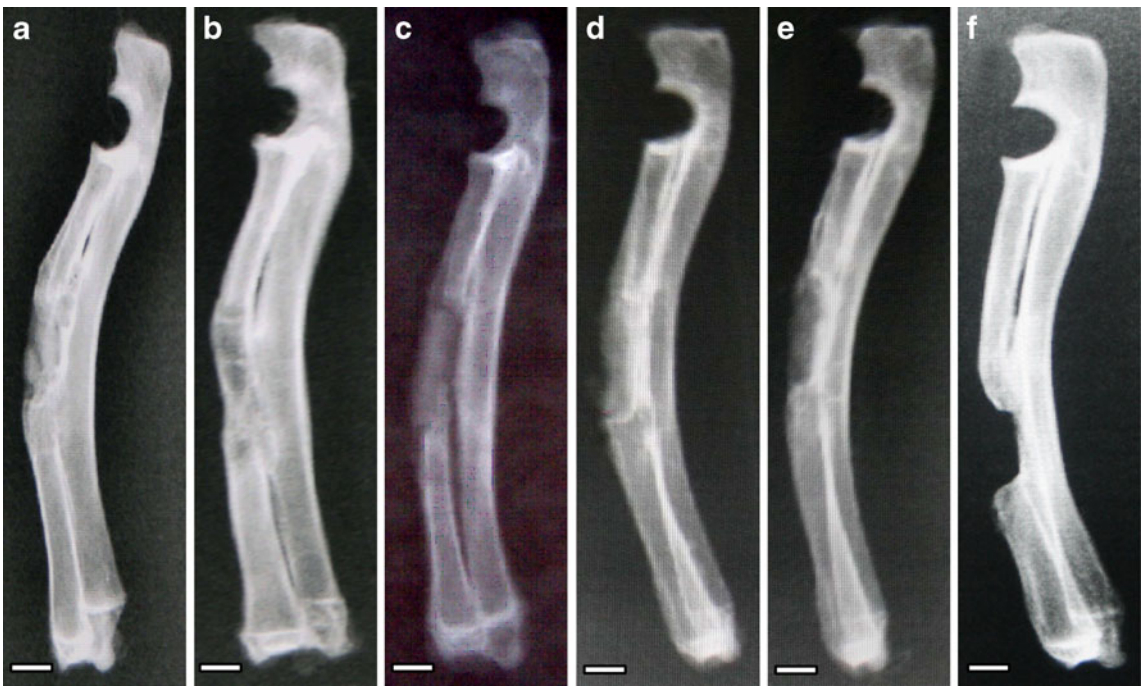

Fig. 4 Radiographic results after implantation of different groups into radial bone defect including hBMP2/rASCs-nHA/RHLC/PLA (group 1) at six weeks (**a**) and 12 weeks (**b**), rASCs-nHA/RHLC/PLA (group 2) at six weeks (**c**) and 12 weeks (**d**), nHA/RHLC/PLA (group 3) at 12 weeks (**e**) and blank control (group 4) (**f**) at 12 weeks. Scale bar 0.5 cm

image scoring suggested that the bone formation in group 1 was statistically superior to that in group 2 ($p<0.05$; Table 2). In the control group treated with scaffold alone, no radiographic appearance of bone formation was observed (Fig. 4e) and the critical defect site was not healed after 12 weeks in the untreated controls (Fig. 4f).

Histological analyses

In group 1, bone tissue was evenly distributed in the scaffold pores after six weeks (Fig. 5a). Bony union was achieved and the medullary cavity was recanalised after 12 weeks; at this time, the scaffold was almost completely degraded (Fig. 5b). In group 2, new bone was observed in a few pores of the scaffold after six weeks (Fig. 5c), and the medullary cavity near the cutting ends was sealed with bone cortex after 12 weeks (Fig. 5d) with connective tissue growth into the pores of scaffold (Fig. 5c, d). In group 3, no bone formation was observed, even at 12 weeks post-surgery (data not shown).

After six weeks, the bone forming area was 46.32± 1.38% in group 1; this increased to 97.25±2.06% at 12 weeks post-surgery (Fig. 6). Both values were significantly higher than for group 2 at six weeks (10.24±1.12%) and 12 weeks (13.72±1.32%) ($p< 0.05$). The residual scaffold occupation area decreased in a corresponding fashion. The material degradation rate was significantly different among groups 1, 2, and 3 (Fig. 7). The most rapid degradation was observed in group 1, then group 2, and then group 3 ($p<0.05$).

Discussion

In this study, autologous rASCs were transduced with Ad-hBMP2 and then combined with a novel nHA/RHLC/PLA scaffold. Good osteogenic potency of rASCs has been demonstrated after transduction with hBMP2, and a critical-sized bone defect has been successfully repaired 12 weeks postoperatively.

Bone tissue engineering requires three key elements: bone-forming cells, osteoinductive growth factors, and porous scaffolds. Porous scaffolds provide an adequate microenvironment for seed cells to proliferate and differentiate and osteoinductive growth factors promote committed cells to differentiate towards osteogenesis. Several cell sources have been used to fabricate bioengineering constructions, including osteoblasts and MSCs. Osteoblasts possess widely-accepted ossification capacity. But limited cell availability, poor in vitro proliferation, and donor site morbidity greatly limits its clinical use. Ideal seed cells can be characterised by easy harvest, rapid proliferation, and good differentiation when cultured in vitro. Nowadays, as demonstrated in various reports, MSCs have been proven to possess similar properties and are thereby extensively used in cell-based bone tissue engineering.

Bone defect repair usually requires a large number of MSCs to be incorporated into biomaterials so as to produce adequate new bony tissue. Nevertheless, the accurate cell number is highly uncertain. Many aspects could directly influence the in vivo osteogenesis of bioengineering constructions, including the in vitro culture conditions and different lots of harvested cells, highly individualised scaffold structure, and the diversified cell seeding efficiency (cell adhered to scaffold/total seeding cells). Consequently, as indicated by various studies, the therapeutic effects of purely cell-based bioengineering composites for bone defect repair have been controversial. Several reports indicated that MSCs combined with appropriated biomaterials could heal critical-sized bone defects [1–3]. However, similar to the results of the non-transduced rASCs group in this report, some other reports demonstrated opposite findings. Li et al. and Peterson et al. demonstrated failed repair of bone defects in canine and rat models by using ASCs incorporated with biomaterials [20, 21]. Cuomo et al. observed that MSCs-enriched bone marrow aspirate mixed with demineralised bone matrix could not result in reliable healing of critical-sized bone defects [22]. To reduce those latent uncertainties, methods to increase cell number in scaffolds, such as retainment of seeding cells by semi-solid hydrogels [23, 24] or surface modification of the scaffolds to increase cell affinity, have been attempted [25, 26]. Although the reinforced ossification effects were manifest and confirmative, preparation procedures are time-consuming, accompanied by increased potential risks such as infection, loss of pluripotency, and decrease of osteogenic potential for MSCs after multiple passages [27, 28].

Use of osteoinductive growth factors hold promise. Bone morphogenetic proteins (BMPs) have demonstrated osteoinductive and osteogenic potential in animal and clinical studies, and use of recombinant BMP-2 has been approved by the Food and Drug Administration (FDA) for spinal fusion treatment. However, the results of clinical trials were not as good as those of reported animal research. On the one hand, high doses are required for the BMP to be effective in clinical cases [29, 30], which may be due to a

Table 2 Radiographic scores at different time points

Time (weeks)	Group 1	Group 2	Group 3
6	6.33*	0.83**	0
12	11.67*	1**	0

* $p<0.05$ compared with groups 2 and 3

** $p<0.05$ compared with group 3

Significance determined by Mann-Whitney U test

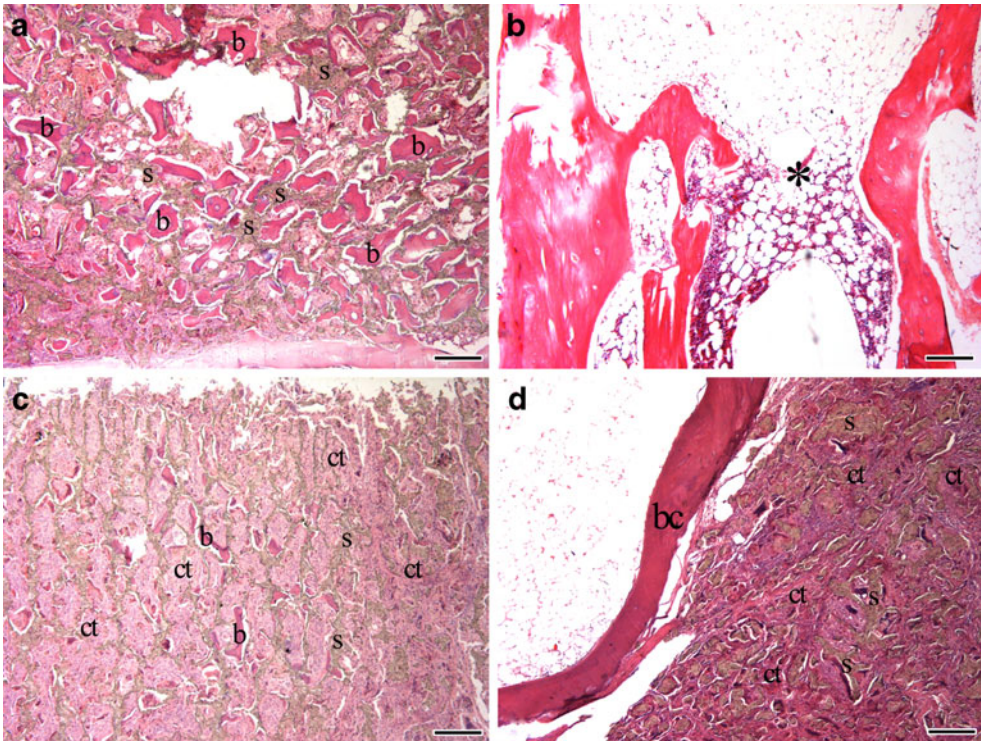

Fig. 5 Histological analyses of hBMP2/rASCs-nHA/RHLC/PLA (group 1) and rASCs-nHA/RHLC/PLA (group 2) at six weeks (**a**, **c**) and 12 weeks (**b**, **d**). Scale bar 500 μm. *b* new bone tissue, *s* residual scaffold (*grey color*), *ct* connective tissue, *bc* bone cortex* Recanalised medullary cavity

variation in the ability of therapeutic doses of BMPs to stimulate alkaline phosphatase expression of individual human MSCs and subsequent lack of control of osteoid mineralisation [31]. On the other hand, recombinant BMP-2 is expensive and there are concerns about potential oncogenic effects, especially if redosing is necessary [21]. Unlike direct administration of a therapeutic BMP protein, gene therapy allows the targeted delivery of BMP to specific cells and thus not only increases the efficacy of osteoinductive cytokine transmission to a specific target site, but also maximally stimulates local osteogenesis [32]. Adenoviral vector systems have been widely used to deliver target genes into MSCs. Adenoviral vectors are efficient, can be produced in high titres, achieve high levels of expression following transduction, and can transfer genes to both dividing and nondividing cells [33]. In this study, rASCs were transfected with a replication defective adenovirus-mediated BMP2 gene

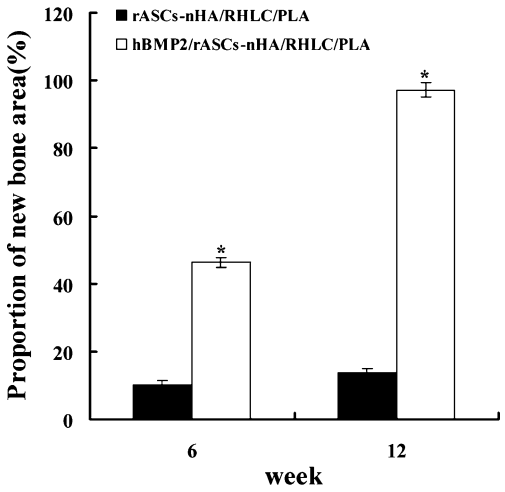

Fig. 6 Proportion of new bone area of hBMP2/rASCs-nHA/RHLC/PLA (group 1) and rASCs-nHA/RHLC/PLA (group 2) at six weeks and 12 weeks. *$p<0.05$ was statistically significant compared with rASCs-nHA/RHLC/PLA (group 2)

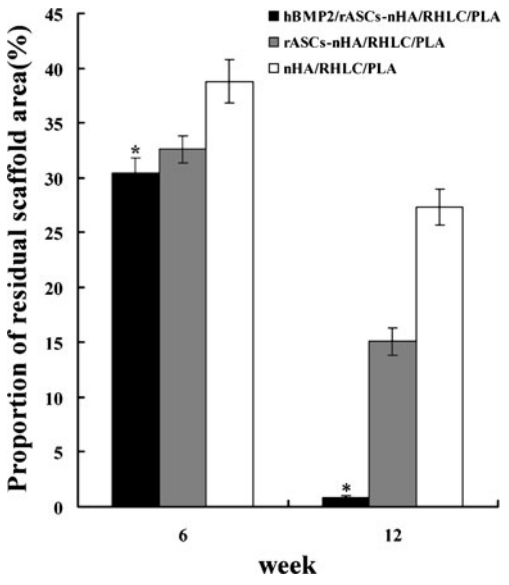

Fig. 7 Proportion of residual scaffold area of hBMP2/rASCs-nHA/RHLC/PLA (group 1), rASCs-nHA/RHLC/PLA (group 2) and nHA/RHLC/PLA (group 3) at six weeks and 12 weeks. *$p<0.05$ was statistically significant compared with rASCs-nHA/RHLC/PLA (group 2) and nHA/RHLC/PLA (group 3)

(Ad-hBMP2). Real-time RT-PCR results demonstrated continuously enhanced expression of osteogenic specific genes in the ASCs after transduction. Although our results were encouraging, adenoviral vectors have some drawbacks such as transient transgene expression, a host immune response which may exert unfavourable influence on the osteogenesis to some extent. Recent studies suggest that the adeno-associated viral vectors (AAV) may be more suitable for gene delivery in bone tissue engineering since they are non-pathogenic, non-immunogenic, and are able to infect a wide variety of dividing and non-dividing cells [32, 34, 35]. Further research will focus on the use of AAV in our group.

The three-dimensional (3D) porous scaffold is another crucial element during bone tissue engineering fabrication. Suitable biomaterials should mimic the microstructure of cancellous bone and be nonimmunogenic, biodegradable, biocompatible, and osteoconductive. In addition, high porosity for seed cell diffusion, differentiation and vasculature ingrowth is necessary. The biomaterial we used in this report was made up of nano-hydroxyapatite (nHA), recombinant human-like collagen (RHLC) and poly(lactic acid) (PLA). The nHA/RHLC was first fabricated and then mixed with PLA at a 1:1 weight ratio to produce nHA/RHLC/PLA composite [14]. The structure of mineralised fibril bundles of nHA/RHLC was similar to mineralised collagen of natural bone [15], and the RHLC had the same effect as animal-sourced collagen in directing growth of HA nanocrystals in vitro in the form of self-assembly of nanofibrils [16] while refraining from potential antigenicity and immunogenicity of xenogenic collagen. The addition of PLA reinforced the mechanical properties and porous structure of the scaffold. X-ray diffraction confirmed that the broadening of the diffraction peaks of nHA/RHLC/PLA characterised by the small grain size and low crystallinity is very similar to the pattern of natural bone [14]. After combining bone marrow or osteoinductive growth factors with nHA/RHLC/PLA scaffold, apparent bone formation is observed in ectopic or orthotopic sites and the scaffold degrades accordingly [14, 17]. As shown by SEM, when the transduced rASCs were combined with the novel nHA/RHLC/PLA scaffold, the rASCs in the scaffold exhibited favourable growth. After implantation into the bone defect site, the scaffold degradation rate corresponded to the rate of bony tissue formation. This is important since suitable biomaterial of bone tissue engineering should degrade promptly to provide enough space for continuous ingrowth of new bone tissue. Defects treated with hBMP2/rASCs-nHA/RHLC/PLA biocomposite were completely healed and the scaffold completely degraded based on radiographic and histological data after 12 weeks. In the control group treated with scaffold alone, no healing was observed.

This report demonstrates the utility of a new bone tissue engineering construct based on hBMP2 gene-modified ASCs and the nHA/RHLC/PLA scaffold. The findings indicate favourable osteogenesis in vitro and bone formation with relatively short repair duration in vivo. The novel therapeutic strategy represents an effective and feasible technique and may provide a promising method for orthopaedic surgeons to treat bone loss problems in human cases.

References

1. Yuan J, Cui L, Zhang WJ, Liu W, Cao Y (2007) Repair of canine mandibular bone defects with bone marrow stromal cells and porous beta-tricalcium phosphate. Biomaterials 28:1005–1013
2. Di Bella C, Farlie P, Penington AJ (2008) Bone regeneration in a rabbit critical-sized skull defect using autologous adipose-derived cells. Tissue Eng Part A 14:483–490
3. Yoon E, Dhar S, Chun DE, Gharibjanian NA, Evans GR (2007) In vivo osteogenic potential of human adipose-derived stem cells/poly lactide-co-glycolic acid constructs for bone regeneration in a rat critical-sized calvarial defect model. Tissue Eng 13:619–627
4. De Ugarte DA, Morizono K, Elbarbary A, Alfonso Z, Zuk PA, Zhu M, Dragoo JL, Ashjian P, Thomas B, Benhaim P, Chen I, Fraser J, Hedrick MH (2003) Comparison of multi-lineage cells from human adipose tissue and bone marrow. Cells Tissues Organs 174:101–109
5. Hicok KC, Du Laney TV, Zhou YS, Halvorsen YD, Hitt DC, Cooper LF, Gimble JM (2004) Human adipose-derived adult stem cells produce osteoid in vivo. Tissue Eng 10(3–4):371–380
6. Mauney JR, Kirker-Head C, Abrahamson L, Gronowicz G, Volloch V, Kaplan DL (2006) Matrix-mediated retention of in vitro osteogenic differentiation potential and in vivo bone-forming capacity by human adult bone marrow-derived mesenchymal stem cells during ex vivo expansion. J Biomed Mater Res A 79:464–475
7. Dragoo JL, Choi JY, Lieberman JR, Huang J, Zuk PA, Zhang J, Hedrick MH, Benhaim P (2003) Bone induction by BMP-2 transduced stem cells derived from human fat. J Orthop Res 21:622–629
8. Turgeman G, Aslan H, Gazit Z, Gazit D (2002) Cell-mediated gene therapy for bone formation and regeneration. Curr Opin Mol Ther 4:390–394
9. Wang M (2003) Developing bioactive composite materials for tissue replacement. Biomaterials 24:2133–2251
10. Van Landuyt P, Li F, Keustermans JP, Streydio JM, Delannay F, Munting E (1995) The influence of high sintering temperatures on the mechanical properties of hydroxyapatite. J Mater Sci Mater Med 6:8–13
11. Zhang PB, Hong ZK, Yu T, Chen XS, Jing XB (2009) In vivo mineralization and osteogenesis of nanocomposite scaffold of poly (lactide-co-glycolide) and hydroxyapatite surface-grafted with poly(L-lactide). Biomaterials 30:58–70
12. Webster TJ, Ergun C, Doremus RH, Siegel RW, Bizios R (2000) Specific proteins mediate enhanced osteoblast adhesion on nanophase ceramics. J Biomed Mater Res 51:475–483
13. Webster TJ, Siegel RW, Bizios R (1999) Osteoblast adhesion on nanophase ceramics. Biomaterials 20:1221–1227
14. Wang Y, Cui FZ, Hu K, Zhu XD, Fan DD (2008) Bone regeneration by using scaffold based on mineralized recombinant collagen. J Biomed Mater Res B Appl Biomater 86:29–35
15. Zhai Y, Cui FZ (2006) Recombinant human-like collagen directed growth of hydroxyapatite nanocrystals. J Cryst Growth 291:202–206
16. Wang Y, Cui FZ, Zhai Y, Wang XM, Kong XD, Fan DD (2006) Investigations of the initial stage of recombinant human-like collagen mineralization. Mat Sci Eng 26:635–638

17. Wu B, Zheng Q, Guo X, Wu Y, Wang Y, Cui F (2008) Preparation and ectopic osteogenesis in vivo of scaffold based on mineralized recombinant human-like collagen loaded with synthetic BMP-2-derived peptide. Biomed Mater 3:44111
18. Hao W, Hu YY, Wei YY, Pang L, Lv R, Bai JP, Xiong Z, Jiang M (2008) Collagen I gel can facilitate homogenous bone formation of adipose-derived stem cells in PLGA-beta-TCP scaffold. Cells Tissues Organs 187:89–102
19. Livak KJ, Schmittgen TD (2001) Analysis of relative gene expression data using real-time quantitative PCR and the 2(-delta delta C(T)) method. Methods 25:402–408
20. Li H, Dai K, Tang T, Zhang X, Yan M, Lou J (2007) Bone regeneration by implantation of adipose-derived stromal cells expressing BMP-2. Biochem Biophys Res Commun 356:836–842
21. Peterson B, Zhang J, Iglesias R, Kabo M, Hedrick M, Benhaim P, Lieberman JR (2005) Healing of critically sized femoral defects, using genetically modified mesenchymal stem cells from human adipose tissue. Tissue Eng 11:120–129
22. Cuomo AV, Virk M, Petrigliano F, Morgan EF, Lieberman JR (2009) Mesenchymal stem cell concentration and bone repair: potential pitfalls from bench to bedside. J Bone Joint Surg Am 91:1073–1083
23. Schantz JT, Hutmacher DW, Lam CX, Brinkmann M, Wong KM, Lim TC, Chou N, Guldberg RE, Teoh SH (2003) Repair of calvarial defects with customised tissue-engineered bone grafts II. Evaluation of cellular efficiency and efficacy in vivo. Tissue Eng 9(Suppl 1):S127–S139
24. Weinand C, Pomerantseva I, Neville CM, Gupta R, Weinberg E, Madisch I, Shapiro F, Abukawa H, Troulis MJ, Vacanti JP (2006) Hydrogel-beta-TCP scaffolds and stem cells for tissue engineering bone. Bone 38:555–563
25. Hauser J, Zietlow J, Köller M, Esenwein SA, Halfmann H, Awakowicz P, Steinau HU (2009) Enhanced cell adhesion to silicone implant material through plasma surface modification. J Mater Sci Mater Med 20(12):2541–2548. doi:10.1007/s10856-009-3826-x
26. Pang L, Hu YY, Yan YN, Liu L, Xiong Z, Wei YY, Bai JP (2007) Surface modification of PLGA/β-TCP scaffold for bone tissue engineering: hybridization with collagen and apatite. Surf Coat Technol 201:9549–9557
27. Digirolamo CM, Stokes D, Colter D, Phinney DG, Class R, Prockop DJ (1999) Propagation and senescence of human marrow stromal cells in culture: a simple colony-forming assay identifies samples with the greatest potential to propagate and differentiate. Br J Haematol 107:275–281
28. Sugiura F, Kitoh H, Ishiguro N (2004) Osteogenic potential of rat mesenchymal stem cells after several passages. Biochem Biophys Res Commun 316:233–239
29. Boden SD, Kang J, Sandhu H, Heller JG (2002) Use of recombinant human bone morphogenetic protein-2 to achieve posterolateral lumbar spine fusion in humans: a prospective, randomized clinical pilot trial: 2002 Volvo Award in clinical studies. Spine (Phila Pa 1976) 27:2662–2673
30. Sakou T (1998) Bone morphogenetic proteins: from basic studies to clinical approaches. Bone 22:591–603
31. Diefenderfer DL, Osyczka AM, Garino JP, Leboy PS (2003) Regulation of BMP-induced transcription in cultured human bone marrow stromal cells. J Bone Jt Surg Am 85-A(Suppl 3):19–28
32. Luk KD, Chen Y, Cheung KM, Kung HF, Lu WW, Leong JC (2003) Adeno-associated virus-mediated bone morphogenetic protein-4 gene therapy for in vivo bone formation. Biochem Biophys Res Commun 308:636–645
33. Crystal RG (1995) Transfer of genes to humans: early lessons and obstacles to success. Science 270:404–410
34. Nasu T, Ito H, Tsutsumi R, Kitaori T, Takemoto M, Schwarz EM, Nakamura T (2009) Biological activation of bone-related biomaterials by recombinant adeno-associated virus vector. J Orthop Res 27:1162–1168
35. Yazici C, Yanoso L, Xie C, Reynolds DG, Samulski RJ, Samulski J, Yannariello-Brown J, Gertzman AA, Zhang X, Awad HA, Schwarz EM (2008) The effect of surface demineralization of cortical bone allograft on the properties of recombinant adeno-associated virus coatings. Biomaterials 29:3882–3387